Active connectors for microfluidic drops on demand

2009 New J. Phys. 11 075027

(http://iopscience.iop.org/1367-2630/11/7/075027)

New Journal of Physics
The open-access journal for physics

Active connectors for microfluidic drops on demand

Jean-Christophe Galas[1], **Denis Bartolo**[2] **and Vincent Studer**[1]

[1] Laboratoire de Neurobiologie, ESPCI-CNRS UMR 7637,
10 rue Vauquelin 75231 Paris cedex 05, France
[2] PMMH-ESPCI-CNRS UMR 7636-Université Paris 6-Université Paris 7,
10 rue Vauquelin 75231 Paris cedex 05, France
E-mail: jean-christophe.galas@espci.fr, denis.bartolo@espci.fr and
vincent.studer@espci.fr

New Journal of Physics **11** (2009) 075027 (11pp)
Received 3 February 2009
Published 31 July 2009
Online at http://www.njp.org/
doi:10.1088/1367-2630/11/7/075027

Abstract. We introduce a simple and versatile microfluidic drop-on-demand solution that enables independent and dynamical control of both the drop size and the drop production rate. To do so, we combine a standard microfluidic T-junction and a novel active switching component that connects the microfluidic channel to the macroscopic liquid reservoirs. Firstly, we explain how to make this simple but accurate drop-on-demand device. Secondly, we carefully characterize its dynamic response and its range of operations. Finally, we show how to generate complex two-dimensional drop patterns dynamically in single or multiple synchronized drop-on-demand devices.

Contents

1. Introduction

Droplet microfluidics enables us to create and manipulate independent picoliter reactors at a high rate inside microfluidic circuits. As a result, it is considered to be a powerful tool for high-throughput approaches to drug discovery, particle synthesis or parallel monitoring of (bio)chemical reactions [1]. In most of the current applications, periodic trains of droplets are spontaneously created at the junction of two streams of immiscible fluids. It is thus very simple to produce highly monodisperse droplets with diameters ranging between 10 and 100 μm at rates ranging from 1 Hz to 1 kHz. Nevertheless, in practice, it is impossible to achieve independent control of the drop size, spacing and velocity. For instance, making 50 μm droplet trains with a spacing of 500 μm at a rate of 10 drops per second would require a very fine tuning of the channel geometry and of the inlet pressures or flow rates. This is usually achieved by a tedious and time-consuming trial-and-error procedure. In a different context, the integration of active components can improve the dynamic control of microfluidic flows [2, 3]. In particular, valves greatly facilitate the temporal modulations of liquid compositions and of flow rates. In addition, they can be used to control independently a large number of reagents [3]. However, attempts to use valves in order to enhance the control of droplet creation and manipulation have been scarce [4]–[8]. Although these recent works improve the control over drop production, they do not provide a full and simple drop-on-demand solution.

In this paper, we introduce a simple generic device to control accurately and independently drop size, speed and spacing over a large range of operation. This solution relies on an active microfluidic connector, which includes a single pneumatic Quake valve [9] to regulate the flow of the dispersed phase. When the valve is open and closed, a single drop is produced and the size of this drop is controlled by the opening time of the valve.

This paper is organized as follows: firstly, we show how to fabricate active connectors (ACs) between microfluidic circuits and macroscopic liquid reservoirs. Secondly, we explain how to use these connectors to control droplet formation and present a comprehensive characterization of this drop-on-demand component. Thirdly, we explain how to take advantage of the fast dynamic response of the AC to generate non-periodic sequences of droplets of controlled size and separation. Finally, we show how to very accurately synchronize several ACs and demonstrate this important advantage by generating dynamically two-dimensional complex patterns of droplets.

2. Fabrication of ACs and a drop-on-demand device

The AC consists in a small (typically $5 \times 5 \times 5$ mm) PDMS (polydimethylsiloxane) cube containing a short straight microchannel and a single pneumatic Quake valve. This device is arguably the simplest multilayer soft lithographic device [9]. A detailed description of all the materials and methods we used is provided in the experimental methods section. Briefly, the principle of the AC is sketched in figure 1. It is composed of two straight perpendicular PDMS channels bound one on top of the other and separated by a thin PDMS layer. The lower channel is bound to the surface of a microfluidic device and connects any of its inlets (or outlets) to an external liquid reservoir. By increasing the pressure inside the upper channel (control channel), the thin membrane buckles, closes the channel underneath and in turn isolates the microfluidic circuit from the reservoir. The upper control channel is filled with water, and the lower channel is filled with the fluid we want to regulate the flow. The AC is actuated by a computer-controlled air

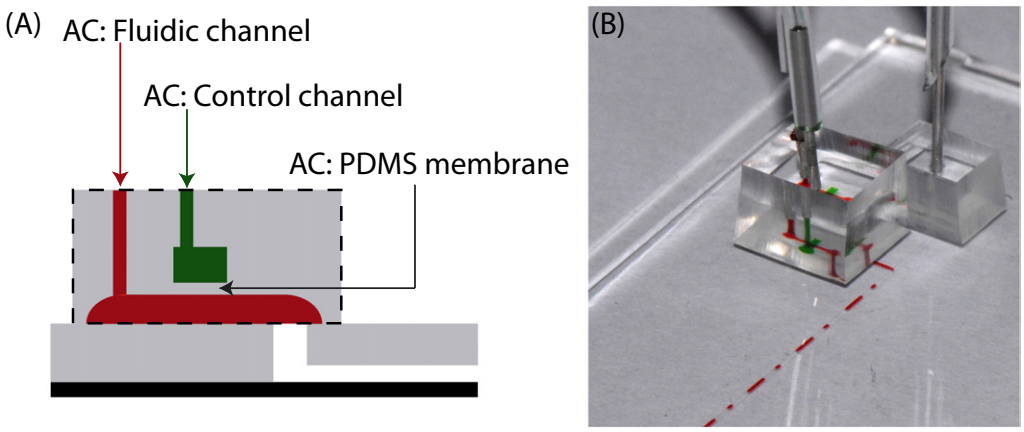

Figure 1. (A) Sketch of an AC bound to a microfluidic channel, cross-sectional view. (B) Picture of a T-junction drop-on-demand device. Drops of water and red dye are produced in mineral oil. The device is made of PDMS. The mineral oil is injected in a passive PDMS connector (rightmost PDMS cube). The water solution is injected through an AC (leftmost PDMS cube). The control channel is pressurized with a solution of water colored with a green food dye. Note that the variations of the drop size are controlled by the AC.

pressure source. The resulting ACs combine the advantage of Quake valves and the simplicity of use of PDMS for external macroscopic connections [10]. More precisely, they display a small footprint (similar to commercial connectors), a small inner volume ($\sim$10 nl), a small displaced volume ($<$1 nl), a fast response time ($\sim$10 ms), high reproducibility and computer-controlled switching. We add that only the connector must be made of PDMS. Indeed, we successfully bound PDMS connectors to glass, and several types of photocurable polymers by using conventional oxygen plasma bonding. This is a great advantage in the context of droplet microfluidics since the range of available surface chemistry is significantly increased. It is also worth noting that the design of the microfluidic circuit is not constrained by the presence of the active component.

We now explain how to use a single AC to make a drop-on-demand device based on a T-junction circuit (figure 1(B)). Most of the experiments have been carried out using microfluidic stickers made of NOA81 photocurable optical adhesive [11]; again the fabrication of this microchannel is detailed in the experimental methods section. To make water droplets in an oil phase, an AC is bound to the water inlet. The oil phase is a mixture of mineral oil, span 80 (4.5%(vol/vol)), tween 80 (0.4%(vol/vol)) and triton X100 (0.05%(vol/vol)), which strongly inhibits drop coalescence [12]. We forced the two liquids into the system at externally fixed pressures. As shown in figure 2(A), when the AC is closed, the water cannot flow in the device, and so no droplets are produced. When the AC is kept open, drops may or may not be formed, depending on the imposed pressures. In figure 2(B), the flow conditions correspond to a stable coflow. When the AC is opened for a short period of time, a single drop is formed (figure 2(C)). Consequently, drop sequences are produced by imposing computer-controlled pressure pulses on the AC (figure 2(D)). We discuss this important application in the next two sections.

In all the results presented, we controlled water flows with the PDMS AC. If one is interested in making a direct oil in water emulsion, an organic liquid has to flow in the PDMS valve. This may be a major problem when dealing with solvents that strongly swell the silicon

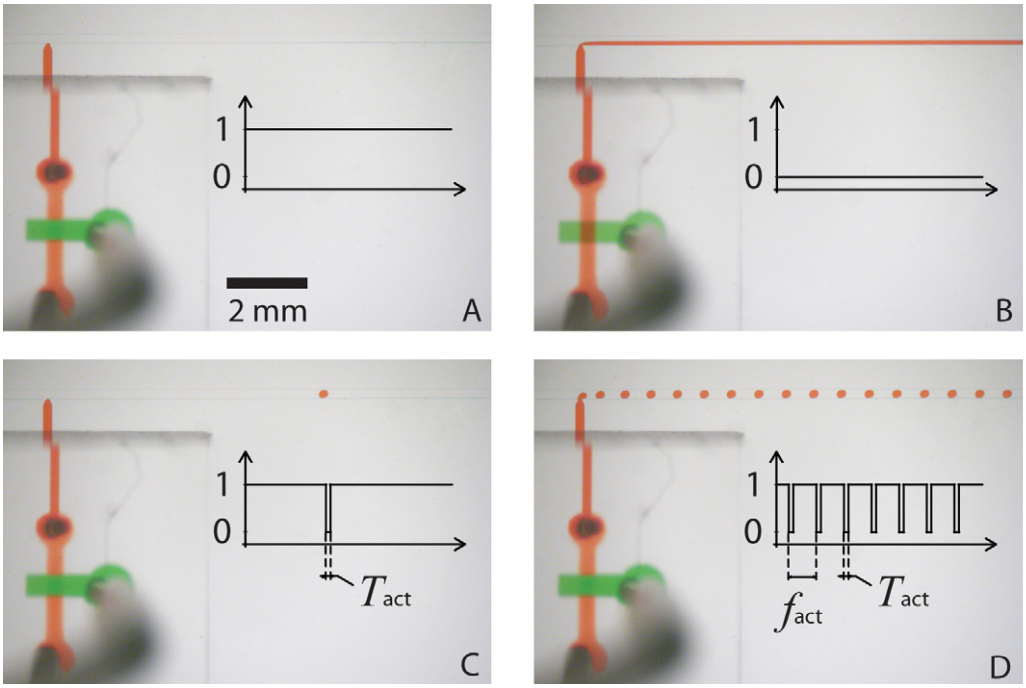

Figure 2. Four pictures of the same drop-on-demand device for various actuation signals applied to the AC. An aqueous solution of orange dye is injected at a T-junction in a straight channel filled with mineral oil. The valve of the AC is actuated by pressure pulses in the controlled channel (filled with water and green food dye). On each picture, the graph shows the variations of the actuation pressure with time. Water pressure $P_w = 100$ mbar, oil pressure $P_{oil} = 100$ mbar. (A) AC closed: the water does not flow. (B) AC open: stable coflow of water and oil. (C) The AC is open over a time $T_{act} = 50$ ms: a single drop is produced. (D) The AC is open periodically over a time $T_{act} = 50$ ms: a monodisperse emulsion is produced.

elastomer, thereby preventing the valve from opening and or closing the fluidic channel. To circumvent this difficulty, an obvious option is to use non-swelling solvents such as fluorinated oils. But a more robust solution would be to use a PTFE (polytetrafluoroethylene) pneumatic valve, which is well known to be insensitive to swelling [13].

3. Drop-on-demand device: characteristics and range of operation

We now characterize the dynamic response of this drop production device. We investigate the variations of the drop volume, V_{drop}, and of the drop rate, f_{drop}, for periodic actuations applied to the AC. We denote by T_{act} the duration of a single (squared) pressure pulse and by f_{act} the frequency of the actuation signal. Constant oil and water pressures, P_{oil} and P_w, are imposed. In all that follows we restrict our study to pressures resulting in stable coflows when the AC is kept open (figure 2(B)).

Firstly, we vary f_{act} at fixed $T_{act} = 50$ ms. Up to $f_{act} \sim 20$ Hz, f_{drop} is equal to f_{valve} while V_{drop} remains constant with a very narrow dispersion in size (figure 3(A)). In other words, the

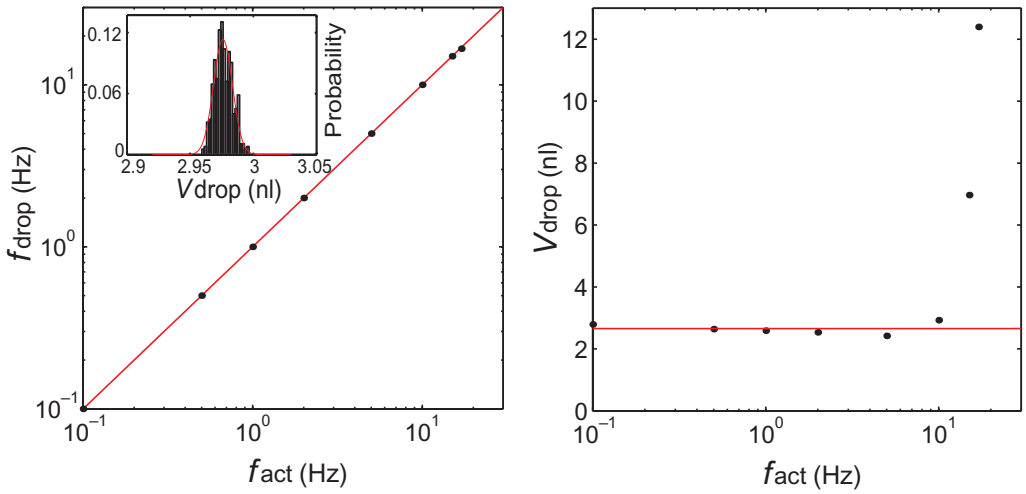

Figure 3. (A) Variations of the drop production rate as a function of the actuation frequency for $T_{act} = 50$ ms, $P_{oil} = 250$ mbar and $P_w = 200$ mbar. Solid line: linear best fit. Inset: probability distribution function of the drop volume for $f_{act} = 10$ Hz, relative mean squared variations: 0.3% deduced from a Gaussian fit. (B) Variations of the drop volume as a function of f_{act} for the same experimental conditions. Solid line: average drop volume for $f_{act} < 10$ Hz. The drop volume depends on f_{act} only above 10 Hz.

production rate can be tuned independently of the drop volume with a single control parameter. This cannot be achieved in passive drop emitters. In practice, the range of operation is here solely limited by the pneumatic valve, which acts as a low-pass filter [14]. The separation between two subsequent pulses, $1/f_{act} - T_{act}$, must be larger than the closing response time of the pneumatic valve. If this condition is not met, the valve cannot fully relax from its open to its closed state, thereby inducing a sharp increase of the drop volume with the actuation frequency (figure 3(B)). Conversely, the partial closing of the valve only weakly alters the variations of f_{drop}, which remains locked on f_{act}. We should note that the response of the drop emitter to the weak amplitude perturbations induced by the partial closing of the valve has been extensively studied in [15]. In this paper, the authors studied the highly nonlinear response of a flow rate-controlled drop emitter to the perturbations induced by the oscillations of an integrated Quake valve. Since the dispersed phase was injected at a constant flow rate, the pressure-controlled valve could not be fully closed and only weakly modulated the local pressure field.

Secondly, we vary T_{act} at fixed $f_{act} = 5$ Hz and measure both f_{drop} and V_{drop}. The volume of the droplets increases with T_{act} while f_{drop} remains constant as T_{act} remains higher than 40 ms (figure 4 and inset). Consequently, the drop volume can be easily varied independently of the drop production rate with a single control parameter: T_{act}. One would expect the drop volume to scale as $V_{drop} \sim Q_w T_{open}$, with T_{open} the time during which the valve is open and the water flows in the channel at a rate Q_w. In figure 4(A), we observe an affine increase of V_{drop} with T_{act}. This apparent contradiction is in fact consistent with the finite (opening) response time of the valve τ_v. A rough estimate of T_{open} is given by $T_{open} \sim T_{act} - \tau_v$. The intersection of the affine fit with the $V_{drop} = 0$ axis yields $\tau_v \sim 42$ ms, which is indeed the typical order of magnitude reported for the opening time of a similar Quake valve [14]. Importantly, for actuation times smaller

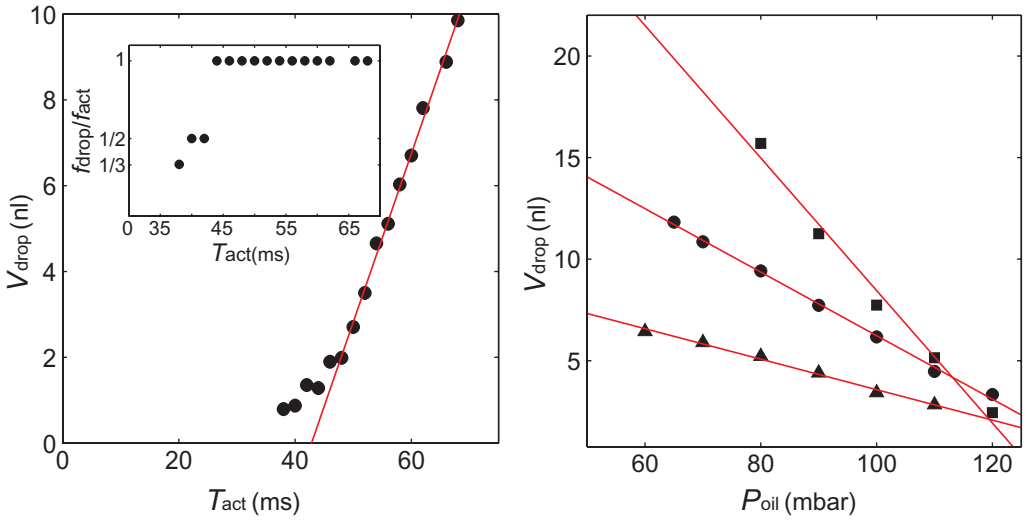

Figure 4. (A) Drop volume as a function of opening time T_{act} at constant $f_{act} = 5$ Hz, $P_{oil} = 250$ mbar and $P_w = 200$ mbar. Solid line: linear best fit for $T_{act} > 45$ ms: $y = 0.1(T_{act} - 42)$. Inset: drop production rate normalized by the actuation frequency. (B) Drop volume versus pressure applied to the oil inlet, P_{oil} at fixed $P_w = 100$ mbar for three different T_{act}: $T_{act} = 50$ ms (triangles), $T_{act} = 90$ ms (circles) and $T_{act} = 150$ ms (squares). Solid lines: best linear fit.

than ~45 ms the production rate is not locked on f_{act} anymore. In figure 4(A) (inset), the drop frequency is seen to be lowered by a factor of two as T_{act} becomes smaller than 45 ms and by a factor of three below 40 ms. To account for these discontinuous deviations from f_{act}, we have to keep in mind that the volume of the drop produced at a T-junction cannot be arbitrarily small, in fact the minimal drop size is set by the channel geometry and is of the order of the water channel width [16, 17]. Since the AC valve is hardly open in the low opening time limit, the volume of water $Q_w T_{open}$ pushed toward the T-junction remains below the minimal dispensing volume and one has to wait for several pressure pulses to produce a single drop. Note that we have implicitly assumed that the water flow rate Q_w is here solely set by external pressures and by channel geometry. In principle, it also depends in a complex way on the number and on the size of the drops in the device [19]. However, these complex corrections to the flow rate do not have any measurable effect on Q_w in our experiments on periodic drop patterns. We will return to this point in the next section.

Thirdly, we vary the pressure P_{oil} and consequently the speed of the droplets. However, increasing P_{oil} we not only increase the oil flow rate Q_{oil} but also reduce the water flow rate Q_w. In turn, Q_{oil} and V_{drop} cannot be varied independently; (figure 4(B)). Nevertheless, our drop-on-demand device enables us to span continuously the (f_{drop}, V_{drop}, Q_{oil}) parameter space (figure 4(B)). This is a major advantage compared to passive drop emitters for which the choice of V_{drop} and f_{drop} would constrain the value of P_{oil} and thus the droplet velocity. Again, this constraint is removed by our drop-on-demand solution, which provides two extra independent parameters T_{act} and f_{act}.

Eventually, we note that the range of operation of this drop-on-demand device could be greatly extended. The minimal drop size is in our case $V_{drop} \sim 200$ pl. Since it scales with the water channel width, it could, in principle, be reduced down to ~10 pl in 10 μm wide channels.

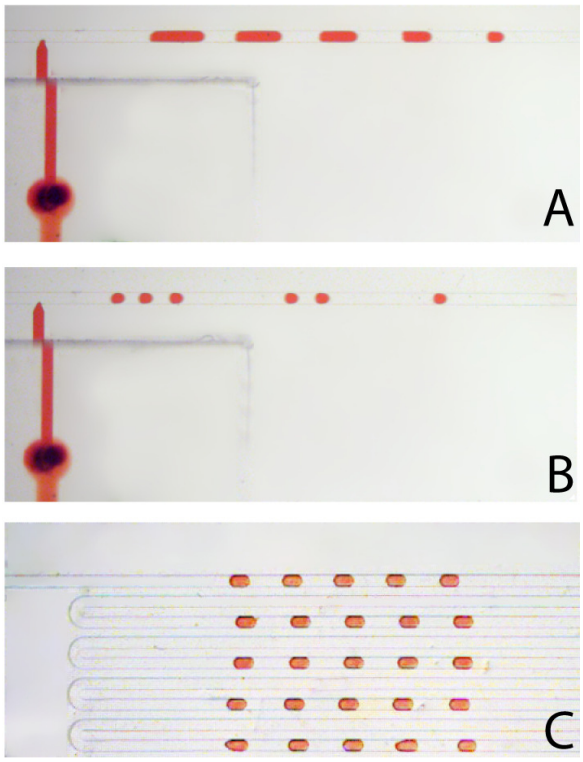

Figure 5. Pictures of non-periodic drop sequences. (A) Decreasing drop size. (B) Drop packets of different length. The two devices are made of PDMS. (C) Squared drop pattern in a 12 cm long channel. The device is made of NOA81 photocurable resin [11]. The channel width is 200 μm.

Furthermore, the shortest pressure pulse ($\sim$40 ms) is solely limited by the response time of the valve in the AC, which could also be greatly reduced, for instance by using a thicker PDMS layer between the control and the fluidic channel [18].

4. Non-periodic drop production and synchronization of multiple drop-on-demand devices

So far we have only reported the production of periodic sequences of identical drops. Thanks to the high dynamic response of the AC described above, our device also enables the production of complex periodic or non-periodic sequences. To emphasize the potential complexity of accessible drop patterns, we provide three specific examples. In figure 4(A), we show a regular sequence of drops having different and controlled size obtained by only varying T_{act} from one drop to the other and keeping f_{act} constant. Conversely, in figure 4(B) the picture corresponds to a sequence where the waiting time between two drop production is varied keeping T_{act} fixed. These two experiments were performed in the same T-junction channel as the one used for figures 4 and 5. To stress the high temporal resolution in the drop release time, we made a drop-on-demand device connected to a long serpentine channel. At fixed Q_{oil} the relative position between the drops is solely set by the separation between the pressure pulses. In turn, at a given time, any spatial pattern can be achieved in the serpentine channel thanks to an accurate

tuning of the pressure pulse sequence. A squared spatial pattern is shown in figure 4(C). It is worth mentioning that the positioning error between the drops sitting in the upper left and lower corner of the square is of the order of 100 μm, which has to be compared with the total length of our pattern: 10 cm. The relative error is as low as 10^{-3}. To achieve this accurate positioning, a two-step process is actually required. We first program the AC to deliver the desired pattern; this results in an ill-defined shape. We measure the position error and adjust the closing times of the AC to compensate for the misalignment. Typically, the corrections we imposed on the drop relative positions are of the order of 1%. By doing so, we reduce this relative error down to 0.1%. The fluctuations in the drop position are due to the local modulations of the oil flow rate along the channel; indeed the opening and the closing of the valve are too accurate to be the limiting factor. The origin of these local velocity fluctuations is twofold: (i) the height of the channel is not perfectly constant over the whole device. Measurements performed with a mechanical profilometer reveal relative height fluctuation of the order of a few percent. Together with the volume conservation constraint, this yields velocity fluctuations of the order of a few percent as well. (ii) As pointed out in the previous section, the hydrodynamic resistance of the circuit depends on the distribution of droplets transported in the channel [19].

This also justifies the assumption we made in the previous section, where we assume that the flow rates are only weakly altered by the structure of the drop pattern in our device. To improve the spatial resolution of the drop positioning, the design of the device could be modified to further reduce the sensitivity on the drop distribution. The ideal case is to have high hydrodynamic resistances, R_w and R_o, at the two inlets. If these two resistances remain higher than that of the output channel where the drops are formed (R), the water and oil flow rates become independent of the drop distribution. Indeed, in the limit $R/R_w \ll 1$ and $R/R_o \ll 1$, the oil and water flow rates are solely set by the external pressures and the channel geometry: $Q_w \sim P_w/R_w$ and $Q_o \sim P_w/R_o$. Moreover, the longer the channel, the more difficult it is to precisely position a drop in a given spatial pattern. An alternative strategy to generate complex spatio-temporal drop sequences thus consists in using several independent drop-on-demand components connected to parallel straight channels. Since the ACs are computer controlled, they can be easily synchronized. By doing so, we manage to display dynamic drop patterns with different drop sizes and spacings as exemplified in figure 6. Eventually, we add that such patterns require an accuracy that cannot be achieved in a PDMS microchannel. The use of a hard NOA81 microfluidics sticker [11] is crucial here to ensure an ultrafast response of the flow rate to pressure changes.

5. Conclusion

We have introduced a connector including a switch function to interface macroscopic liquid reservoirs to microfluidic channels. This new active component simply consists in a single Quake valve embedded in a millimetric PDMS microfluidic connector. The main message of this paper is that the actuation of a standard drop emitter by an AC results in a simple but very efficient drop-on-demand solution for microfluidic applications. Contrary to what is possible in passive droplet microfluidics, this drop-on-demand device allows for accurate, independent and linear control of both the size and the release time of the droplet over a wide range of flow rates. Given the good temporal response of the Quake valves, drops can be produced one at a time or according to complex non-periodic time sequences that can result in controlled but elaborate spatio-temporal drop patterns inside the channels.

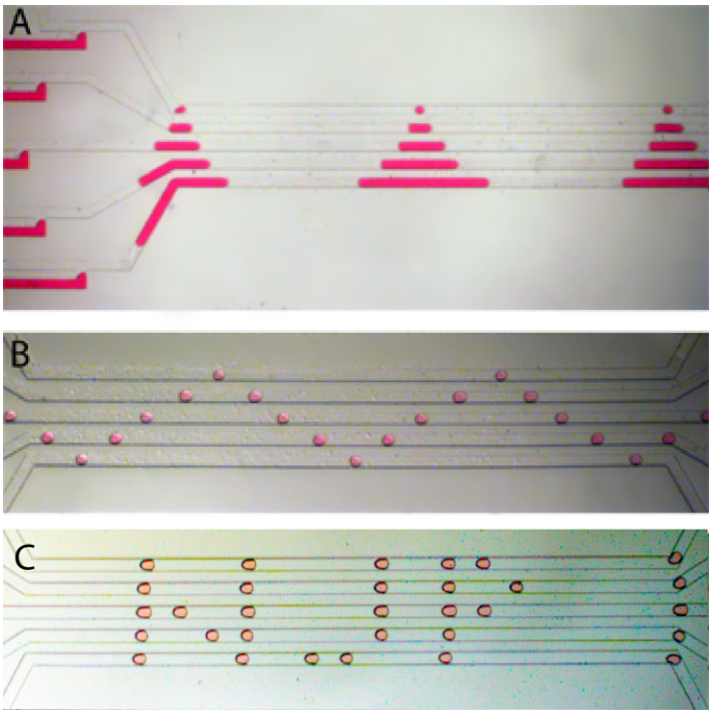

Figure 6. Five disconnected drop-on-demand circuits actuated by five computer-controlled ACs. The circuits are made of NOA81 photocurable resin [11]. The channel width is 200 μm. (A) and (B) Synchronized periodic sequences of drops with regular spacing and size. (C) Example of synchronized non-periodic sequences: the drops form the word 'NJP', which translates at constant speed in the channel (see the movie available at stacks.iop.org/NJP/11/075027/mmedia).

Finally, we should add that the use of ACs is not restricted to droplet microfluidics and ACs have proven to be extremely convenient as a generic connector. For instance (i) they greatly facilitate the filling of microchannels by preventing the cross-contamination of outer liquid reservoirs, (ii) they also enable one to remove or change the liquid inlets and outlets without introducing unwanted bubbles in the device and (iii) they bring an easy solution to stop liquid flows in the device quickly and efficiently.

Acknowledgments

All the primary molds used in the experiments have been made at the ESPCI clean room facility. JCG is supported by ANR grants DROPCELL and BIOPUMP. P Mary is acknowledged for help with the experiments.

Appendix. Experimental methods

A.1. Fabrication of the ACs

The active microfluidic connectors consist of a PDMS cube that includes a single pneumatic Quake valve. They were fabricated by multilayer soft-lithography (MSL): a thin and a thick

layer of PDMS were replicated separately from two photoresist molds. The thick layer was aligned and bound over the thin layer. The thin membrane that separated the upper and lower channels was buckled by applying pressure in the upper channel (the so-called control channel), thus closing the lower channel (fluidic channel) (figure 1). Both the fluidic and the control channels were designed to have an initial width of 500 μm. The molds corresponding to the control channels were fabricated by optical lithography in an 80 μm layer of SU8 2050 photoresist (Microchem). The mold corresponding to the fluidic channels was fabricated in a 40 μm layer of Ma-P 1275 HV resist (Microresist technology) and rounded at 150 °C for 15 min. The fluidic channel layer was obtained by spin coating an RTV 615 PDMS (General Electrics) with a prepolymer/curing agent ratio (w/w) of 20 : 1 at 1000 rpm for 60 s on the corresponding mold. At the same time, replica molding in a 5 mm thick PDMS stamp (prepolymer/curing agent ratio (w/w) of 5 : 1) was performed on the control channel mold in a plastic petri dish. Both PDMS replicas were partially cured at 75 °C for 30 min. Then, the thick PDMS layer was removed from its mold, aligned and placed on the thin one. After bonding at 75 °C for 1 h, the ACs were removed from the mold and access holes were punched with a clean Luer stub adapter (Becton Dickinson).

A.2. Fabrication of microfluidic stickers

Microfluidic sticker channels were made following the procedure described in [11]. Firstly, a two-level PDMS stamp was fabricated by replica molding a two-layer SU8 2050 photoresist mold (Microchem). The first layer containing the microchannel structures was 80 μm high. The second layer contained reservoirs at channel ends and pillars of 160 μm height. Secondly, the PDMS stamp was placed over a flat PDMS layer, and the free space in between these two slabs of PDMS was filled by capillary forces with NOA81 photocurable glue (Norland Optical Adhesive). To speed up the filling we heated the ensemble at 80 °C on a hot plate. The NOA81 was then cured by UV exposure through the transparent PDMS stamp (18 mW cm^{-2} for 17 s). Since oxygen inhibits the free radical polymerization used here to build the polymer network, the permeability to gas of the PDMS ensures that an ultrathin superficial layer of liquid remains uncured. The structured PDMS was then carefully removed in order to keep the NOA81 sticker on the flat PDMS. Then, a drop of NOA81 was deposited on a glass substrate, and a flat PDMS sheet was gently pressed onto the drop to deposit a thin layer of NOA81 on the substrate. This thin layer was cured by UV exposure through the PDMS sheet (18 mW cm^{-2} for 15 s). The flat PDMS layer was removed. The microfluidic sticker was then placed over the NOA81-coated glass substrate and gently pressed on it. A final UV exposure sealed the device (50 mW cm^{-2} for 60 s). Finally, the remaining flat slab of PDMS was removed, thus revealing access holes. Note that the four walls of the channel are all made of the same material.

A.3. Flow control and valve actuation

For precise fluid handling, we used a commercially available pressure controller (MFCS 8C, Fluigent, Paris, France). Typical pressures range from 0 to 500 mbar. For valve actuation, we used a purpose-built controller based on solenoid valves (LHDA 12VDC, Lee Corp.). Typically, air pressures of 1 bar were used to actuate the Quake valve in each AC. Digital signals sent

to the solenoid valves were stored on a digital I/O card (NI PCI-6534, National Instruments) controlled with Matlab software (The MathWorks). The time resolution of these digital control signals is below 1 μs (see also http://thebigone.stanford.edu/foundry/testing/ for details on home made valve controller).

References

[1] Teh S-Y, Lin R, Hung L-H and Lee A P 2008 *Lab Chip* **8** 198
[2] Oh K W and Ahn C H 2006 *J. Micromech. Microeng.* **16** R13
[3] Thorsen T, Maerkl S J and Quake S R 2002 *Science* **298** 580
[4] Abate A R, Romanowsky M B, Agresti J J and Weitz D A 2009 *Appl. Phys. Lett.* **94** 023503
[5] Bransky A, Korin N, Khoury N and Levenberg S 2009 *Lab Chip* **9** 516
[6] Hsiung S K, Chen C T and Lee G B 2006 *J. Micromech. Microeng.* **16** 2403
[7] Lorenz R M, Fiorini G S, Jeffries G D M, Lim D S W, He M Y and Chiu D T 2008 *Anal. Chim. Acta* **630** 124
[8] Baroud C N, Delville J P, Gallaire F and Wunenburger R 2007 *Phys. Rev.* E **75** 046302
[9] Hunger M A, Chou H P, Thorsen T, Scherer A and Quake S R 2000 *Science* **288** 113
[10] Hulme S E, Shevkoplyas S S and Whitesides G M 2008 *Lab Chip* **9** 79
[11] Bartolo D, Degré G, Nghe P and Studer V 2008 *Lab Chip* **8** 274
[12] Williams R, Peisajovich S G, Miller O J, Magdassi S, Tawfik D S and Griffiths A D 2006 *Nat. Methods* **3** 545
[13] Rolland J P, VanDam R M, Schorzman D A, Quake S R and DeSimone J M 2004 *J. Am. Chem. Soc.* **126** 8349
[14] Galas J C, Studer V and Chen Y 2005 *Microelectron. Eng.* **78** 112–7
[15] Willaime H, Barbier V, Kloul L, Maine S and Tabeling P 2006 *Phys. Rev. Lett.* **96** 054501
[16] Garstecki P *et al* 2006 *Lab Chip* **6** 437
[17] Guillot P and Colin A 2005 *Phys. Rev.* E **72** 066301
[18] Goulpeau J, Trouchet D, Ajdari A and Tabeling P 2005 *J. Appl. Phys.* **98** 044914
[19] Labrot V, Schindler M, Guillot P, Colin A and Joanicot M 2009 *Biomicrofluidics* **3** 012804